Chapter 2
Climate Change in Central Asia and Expected Impacts



Bijan Fallah

Abstract Central Asia is a hotspot for climate sensitivity. Its distance from oceans and rugged mountains intensifies atmospheric warming. In this chapter, we present a comprehensive analysis of the region's transitioning climate system, documenting a warming rate that significantly exceeds the global mean–a phenomenon consistent with elevation-dependent warming mechanisms. Observational records indicate that surface air temperatures have already deviated by approximately 1.2 °C relative to the pre-industrial baseline. Furthermore, multi-model ensemble projections under high-emission pathways (Shared Socioeconomic Pathway 5–8.5) suggest a *likely* temperature increase approaching 6 °C by the end of the 21st century (high confidence). Extreme heat is driving a total reorganization of the regional cryosphere and hydrosphere. This transformation poses a systemic risk to the approximately 80 million inhabitants who depend on the delicate balance between glacial melt and river flow. The potential decoupling of water availability from agricultural demand places substantial portions of the regional Gross Domestic Product and millions of livelihoods at risk of displacement and economic destabilization. To quantify these changes, we analyzed 442 climate model simulations from the Coupled Model Intercomparison Project Phase 6 (CMIP6), applied neural network methodologies and regional downscaling (Fallah et al., 2025). Our analysis provides evidence of cascading physical impacts: specifically, the glaciers of the Tien Shan have experienced approximately 27% mass loss since 1961, a degradation that critically compromises the seasonal meltwater buffering capacity essential to 22 million downstream water users. Statistical analysis of extreme events reveals a non-stationarity in recurrence intervals; thermal extremes historically classified as rare events are now observed with increasing frequency. This intensification of hydro-climatic variability is further exemplified by the 2024 Kazakhstan floods–driven by compound mechanisms of rapid snowmelt and soil saturation–which resulted in the displacement of 118,000 individuals, alongside a sevenfold increase in the frequency of multi-year

B. Fallah (✉)
Potsdam Institute for Climate Impact Research (PIK), Member of the Leibniz Association, Potsdam, Germany
e-mail: fallah@pik-potsdam.de

© The Author(s) 2026

I. Didovets et al. (eds.), *Towards Sustainable Future of Central Asia: Analysis of Climate, Resources and Human Security*, Advances in Global Change Research 84,
https://doi.org/10.1007/978-3-032-29989-5_2

meteorological droughts. We conclude that Central Asia is currently undergoing a regime shift from climatic variability to profound transformation, necessitating the urgent deployment of adaptive strategies grounded in robust scientific projections.

Keywords Central Asia · Climate change · CMIP6 · Climate-change adaptation

2.1 Observed Anthropogenic Climate Signals in Central Asia

In July 2023, Tashkent experienced extreme temperatures exceeding 42 °C, a value that statistically deviates significantly from the historical climatological mean (Xinhua, 2023). Attribution analyses utilizing counterfactual climate modeling demonstrate with high confidence that such thermal extremes are no longer stochastic anomalies but are consistent with a shifting probability density function driven by anthropogenic radiative forcing (Fallah & Rostami, 2024). Across Central Asia, the divergence between historical baselines and current observations has shifted from theoretical projection to empirical reality (Fallah et al., 2024). This shift manifests as a decoupling of agricultural phenology from precipitation regimes, an intensification of hydrological extremes ranging from flash floods to meteorological droughts (World Meteorological Organization, 2024), and increasing pressure on transboundary water governance mechanisms.

Climate change–variation in the climate's mean state or in its variability that persists for decades or longer (World Meteorological Organization, 2024)–exerts amplified effects in Central Asia due to the region's high continentality and complex orography. Central Asia brings together vastly different climatic zones (Chen et al., 2019; Fallah, 2024), from the dry Aral Sea littoral to the glacier regions of the Tien Shan and Pamir mountains. This geographic diversity atop an arid-to-semiarid climate makes the system highly sensitive to changes. The region's heavy reliance on seasonal hydrological patterns leaves its population particularly vulnerable to shifts in the interactions among snow, ice, and water systems.

In a previous study (Fallah et al., 2025) we analyzed warming in Central Asia using a dual-layered approach. First, we used large-scale boundary conditions from the Coupled Model Intercomparison Project Phase 6 (CMIP6). Next, we refined them with a neural network-based statistical downscaling technique (Fallah et al., 2025), achieving a spatial resolution of 25 km. This approach shows that Central Asia is warming at about twice the global mean (high confidence). This warming is already visible in several subsystems: shrinking endorheic water bodies, degrading permafrost causing geostructural instability in the cryosphere, and altered discharge in transboundary river basins.

2.1.1 Regional Hydro-Climatic Asymmetries

Kazakhstan, Kyrgyzstan, Tajikistan, Turkmenistan, and Uzbekistan depend on a shared, interdependent water system. Water originates in Kyrgyzstan and Tajikistan, while most arable land and people are found downstream in Uzbekistan, Turkmenistan, and Kazakhstan (Didovets et al., 2024). This setup creates a clear asymmetry in resource control and vulnerability.

The combination of rising temperatures and regional geography is intensifying water-related risks. As glaciers retreat and snowpacks vanish earlier than expected, the resulting shift in river flow triggers spring floods that strain the region's aging infrastructure. Precipitation is shifting from snow to rain, and winters are storing less, undermining hydropower reliability in upstream nations. Our analysis of 442 model simulations shows these hydrological regime changes are already occurring (Fallah et al., 2024).

Observed data show a surface temperature increase of 1.2–1.5 °C over the past century (Fallah et al., 2024). This is enough to induce upslope shifts in ecological niches and change evapotranspiration rates Fallah (2024). Under high-emission scenarios (SSP5-8.5), multi-model ensembles project a temperature increase greater than 4 °C by 2100, with high confidence (Arias et al., 2021). Such a shift could fundamentally disrupt traditional agricultural calendars and water management strategies (Didovets et al., 2024). The predictability of seasonal transitions–especially snowmelt timing and precipitation onset–diminishes under these conditions (Guo et al., 2021).

2.1.2 Paleoclimatic Context and Modern Divergence

Central Asia has a history of significant climatic variability. Now, the speed and magnitude of current changes appear to surpass known Holocene precedents (Chen et al., 2019). Proxy records from the Medieval Climate Anomaly (MCA) indicate periods of increased hydro-climatic variability (Hassanabadi, 2015). These periods were challenging but allowed gradual societal adaptation. The Little Ice Age (LIA), in turn, saw depressed temperatures and severe droughts that influenced settlement and agropastoral strategies. However, these historical anomalies were driven by natural orbital and solar forcing mechanisms. They unfolded over centuries, allowing ecological and societal adjustments (Chen et al., 2019).

Current warming is primarily driven by anthropogenic greenhouse gases and has been occurring over decades. Our scaling analysis of global-to-local teleconnections (Fallah & Saberi, 2016) shows that planetary-scale feedbacks amplify regional warming. The region experiences Elevation-Dependent Warming (EDW), where positive feedbacks, such as the snow-albedo effect and increased downward longwave radiation from water vapor, speed warming at higher altitudes. Meanwhile, expanding arid zones in lowlands risk desertifying steppe ecosystems and reducing arable land (Fallah et al., 2024).

2.1.3 Topographical Controls on Climatic Response

The complex topography of Central Asia (Fig. 2.1) functions as a primary control on the spatial heterogeneity of climate change impacts. The region encompasses a vertical gradient from the Karagiye Depression (–132 m) to the Ismoil Somoni Peak (7,495 m), resulting in stratified climatic zones that respond differently to radiative forcing. The high-mountain cryosphere of the Tien Shan and Pamir ranges, which contains approximately 29,200 km^2 of glacier ice (Farinotti et al., 2015), serves as the hydrological buffer for the region. However, observational data indicate that warming rates in these high-elevation zones have reached 0.55 °C per decade, a rate significantly higher than the global average (Pepin et al., 2022).

This elevational amplification engenders a "climatic paradox": the mountain ranges essential for water storage are experiencing the most rapid thermal forcing, while the downstream lowlands face increasing aridity and evaporative demand. This divergence creates systemic stress on the water-energy-food nexus supporting the region's population. The subsequent sections of this chapter present a synthesis of regional downscaling outputs (Fallah et al., 2025), high-resolution alpine-specific analyses (Fallah, 2024), and event attribution studies (Fallah et al., 2023). By integrat-



Fig. 2.1 Topographic map of the Central Asian domain derived from Digital Elevation Model (DEM) data. The visualization highlights the extreme hypsometric gradient, ranging from sub-sea level depressions in the Caspian basin to high-altitude cryospheric zones (>7000 m) in the Tien Shan and Pamir mountain ranges, which serve as the primary hydrologic source regions

ing these distinct methodological strands, we aim to provide a scientific assessment of the transformation underway, moving beyond broad projections to analyze specific risks to socio-ecological systems and the potential for adaptation in a non-stationary climate.

2.2 Observed Climatic Impacts and Systemic Risks

The amplification of regional warming has transitioned Central Asia into a regime of non-stationary climatic baselines, where the frequency and magnitude of extreme events increasingly exceed historical adaptive capacities. Our analysis of long-term climatological records indicates a statistically significant acceleration in thermal forcing, with a mean surface temperature increase of approximately 1.2 °C observed since the late 19th century (Fallah et al., 2024). This thermodynamic shift has propagated through the coupled earth systems, triggering cascading feedbacks across the cryosphere, hydrosphere, and biosphere.

2.2.1 Cryospheric Degradation and Hydrological Regime Shifts

The high-altitude cryosphere of the Tien Shan and Pamir ranges, historically functioning as the region's primary hydrological buffer, is undergoing rapid structural degradation. These glacial systems, which regulate seasonal discharge by storing winter precipitation and releasing meltwater during the boreal summer, are exhibiting accelerated ablation rates. Since 1961, cumulative mass balance losses are estimated at $27 \pm 15\%$ (Farinotti et al., 2015), a trend that signals the termination of the "Pamir-Karakoram anomaly"–a localized stability previously observed in specific sub-domains–post-2018 (Fallah et al., 2024). Notably, the Fedchenko Glacier, the largest non-polar valley glacier, has experienced a terminal retreat of approximately 1.7 km concomitant with a volumetric loss of 5 km^3, significantly reducing its long-term storage capacity (Lambrecht et al., 2014).

This instability extends to the periglacial domain. Permafrost degradation, characterized by the deepening of the active layer and the thawing of ground ice, is proceeding at vertical rates of 0.5–1.0 m per decade (Fallah, 2024). High-resolution monitoring from analogous high-altitude permafrost systems indicates a doubling of thaw rates in recent decades. The implications are heterogeneous across landforms; rock glaciers (38–60% ice content) and moraine complexes (18–40% ice content) exhibit differential destabilization mechanics (Fallah, 2024). In the northern Tien Shan, this loss of geostructural integrity has compromised critical infrastructure, leading to foundation subsidence and pipeline deformation. Furthermore, the retreat of ice has facilitated the expansion of proglacial lakes; numerous such water bodies

have been identified as hazardous, with aggregate volumes expanding since 1990. These lakes represent significant latent hazards, prone to Glacier Lake Outburst Floods (GLOFs) capable of mobilizing debris flows into densely populated valleys, posing significant risks to downstream populations, as demonstrated by the 1998 Shahimardan outburst event (World Meteorological Organization, 2024).

Concurrently, the seasonal snowpack–critical for soil moisture recharge–exhibits marked temporal contraction. Observational data indicate a reduction in snow cover duration of 15–20 d since 1980, with the onset of the vernal melt shifting 10–15 d earlier (Fallah et al., 2024). This phenological mismatch poses severe risks to agropastoral systems: premature melt results in discharge peaks that precede the growing season's maximum water demand, leading to summer irrigation deficits, while rapid melt rates overwhelm hydraulic infrastructure designed for more gradual flow regimes (Didovets et al., 2024).

2.2.2 Intensification of Hydro-Climatic Extremes

The summer of 2023 was characterized by unprecedented thermal anomalies, with Tashkent recording temperatures exceeding physiological safety thresholds. Attribution studies utilizing Extreme Event Attribution (EEA) methodologies indicate that the probability of such thermal events has increased by a factor of 4.5 due to anthropogenic forcing (Fallah et al., 2023). It is critical to note the distinction in attribution confidence: while thermodynamic extremes (e.g., heatwaves) show a high signal-to-noise ratio directly linked to radiative forcing, dynamic extremes (e.g., convective precipitation) exhibit greater internal variability, though their intensification is consistent with Clausius-Clapeyron scaling (Fallah et al., 2023). The socio-economic impact of this thermal stress was severe, with significant excess mortality and substantial agricultural damages due to crop failure from thermal shock across Central Asia (World Meteorological Organization, 2024).

Conversely, the region has experienced an intensification of pluvial extremes. In April 2024, Kazakhstan faced catastrophic flooding, necessitating the evacuation of 118,000 individuals. This event resulted from a compound driver mechanism: positive surface temperature anomalies (3−8 °C) accelerated snowmelt well above the historical mean, interacting with anomalously high antecedent soil moisture derived from heavy autumnal precipitation. The arrival of an atmospheric river system, delivering precipitation volumes 2 to 4 times above historical norms, exceeded the infiltration capacity of the saturated catchment, leading to widespread inundation and infrastructure damage estimated at several hundred million dollars (World Meteorological Organization, 2024).

While the region faces more frequent heavy rainstorms, the dry periods between them are also becoming longer and more severe. The 2021–2023 drought event represents a synchronized failure of precipitation systems across all five Central Asian nations, a phenomenon unprecedented in the instrumental record. The impacts included widespread water rationing and substantial agricultural losses. Hydrolog-

ical analysis of the Syr Darya basin indicates record-low discharge levels, necessitating emergency transboundary water allocation protocols. Long-term trend analysis reveals a sevenfold increase in drought frequency since 1950, with event duration extending from a historical baseline of 3–6 months to prolonged deficits of 12–18 months (Fallah et al., 2024).

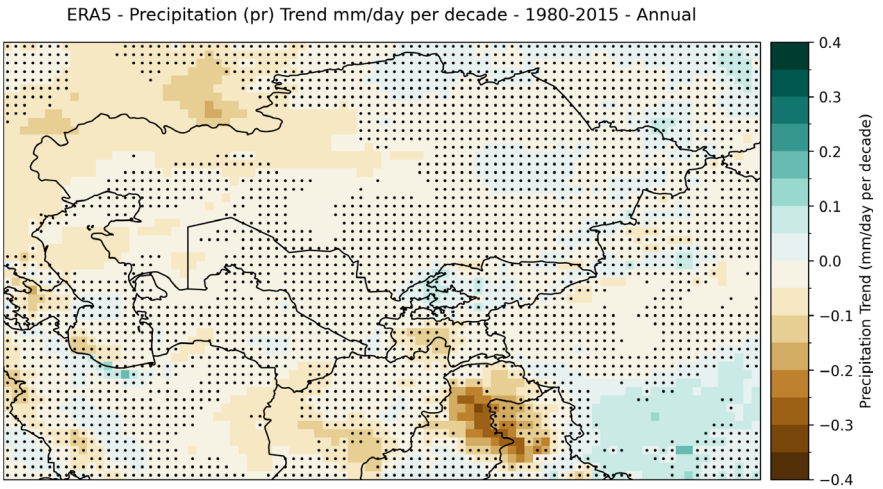
2.2.3 Atmospheric Circulation Dynamics and Synoptic Variability

The synoptic-scale atmospheric circulation patterns governing the Central Asian domain are undergoing significant structural shifts, driven by changes in the global radiative budget. A critical manifestation of this shift is the poleward migration of the subtropical westerly jet stream, the primary mechanism for zonal moisture transport into the region. Observational reanalysis indicates a latitudinal displacement of approximately 1° since 1979 (Fu & Lin, 2011). As winter storms shift northward, the southern mountains are receiving less snow. This disruption to traditional precipitation patterns is creating a significant deficit in the regional water budget.

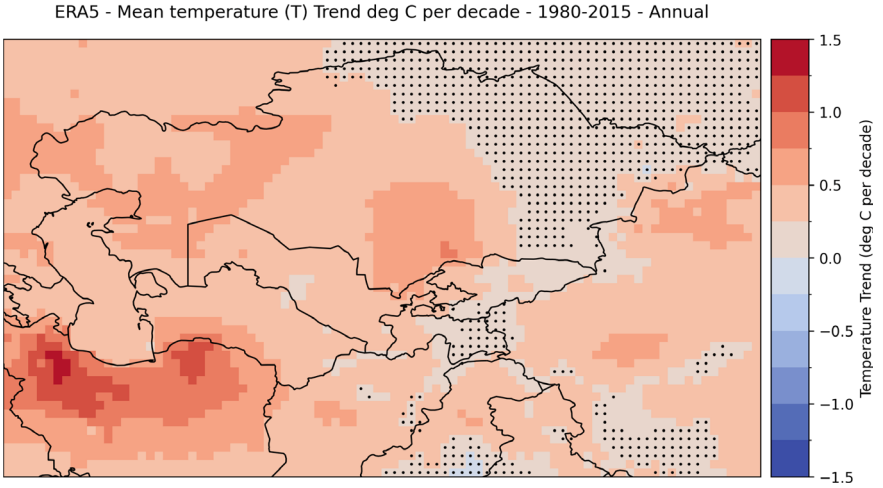
Concurrently, the Siberian High (SH), the semi-permanent anticyclone that dominates winter climatology, has intensified and shifted eastward. This reorganization modulates the advection of continental polar air masses, thereby increasing the variance in winter thermal regimes. The resulting instability manifests as a dipole pattern: intensified cold air outbreaks affect specific sub-regions, while adjacent areas experience positive thermal anomalies driven by reduced anticyclonic blocking (Fallah et al., 2024). This increased stochasticity in frost timing significantly degrades the predictive capacity required for agricultural planning, introducing substantial risk to crop selection and phenological synchronization.

Furthermore, the interaction between the Westerlies and the Indian Summer Monsoon (ISM) is undergoing a phase shift. While the ISM has historically been topographically constrained to the subcontinent, recent evidence suggests an increasing northward penetration into the Central Asian arid zone (Chen et al., 2019). These moisture incursions interact with baroclinic waves embedded in the Westerlies, generating zones of strong convergence and convective instability. Such interactions contribute to an enhancement of extreme precipitation events exceeding 20%, transitioning the region's hydro-climatology towards a regime of heightened non-stationarity and increased convective potential (Zhang & Wang, 2022).

The spatial analysis of these trends (Fig. 2.2) elucidates a marked "climatic dipole" or inequality within the region. A clear latitudinal gradient is observed: northern latitudes exhibit positive precipitation anomalies, whereas southern territories are subject to intensifying aridity. This pattern is superimposed on elevation-dependent warming, in which montane zones experience rapid thermal forcing concurrent with cryospheric depletion (Fallah et al., 2024). The resulting fragmentation of the climatic baseline creates divergent adaptation requirements, with adjacent geopolitical entities



(a) Spatial distribution of linear precipitation trends ($\mathrm{mm\,day^{-1}\,decade^{-1}}$) derived from ERA5 reanalysis data (1980–2015).



(b) Spatial distribution of linear surface temperature trends ($^{\circ}\mathrm{C\,decade^{-1}}$) derived from ERA5 reanalysis data (1980–2015).

Fig. 2.2 Observed climatological trends across the Central Asian domain (1980–2015). Panel (**a**) illustrates the heterogeneity in precipitation anomalies, highlighting the north-south divergence. Panel (**b**) depicts the spatially coherent warming trend, with amplification evident in continental interiors. Data source: ERA5 reanalysis (Hersbach et al., 2020). Dotted areas are not statistically significant

facing opposing hydrological extremes–pluvial versus drought-driven–thereby complicating the development of unified regional adaptation and transboundary cooperation frameworks.

2.2.4 *Projected Warming Trajectories and Bias Correction*

The validation of current-generation climate models against observational records indicates that the trajectory of warming in Central Asia is tracking, and in some metrics exceeding, earlier projections. A comparative analysis of the Coupled Model Intercomparison Project, Phases 6 (CMIP6) and 5 (CMIP5), shows that the latest-generation models exhibit higher Equilibrium Climate Sensitivity (ECS). Specifically, unconstrained projections under the high-forcing Shared Socioeconomic Pathway (SSP5-8.5) suggest a mean regional warming of 6.1 °C by 2100, compared to 5.3 °C under the equivalent Representative Concentration Pathway (RCP8.5) (Fallah et al., 2024). However, it is critical to account for systematic orographic biases; constrained projections that correct for elevation-dependent errors in mountainous terrain indicate a potential reduction in this warming signal (Zhang & Wang, 2022). This variance underscores the need to recognize critical feedback mechanisms that were underrepresented in previous modeling iterations.

The observed surface warming of 1.2 °C relative to pre-industrial baselines has already catalyzed a robust cryospheric response. Observational data indicate a 20% reduction in snow depth over the past 70 years, a trend most pronounced above 3000 m. It is important to note that raw CMIP6 outputs exhibit a positive relative snow cover bias of approximately 52% in these high-elevation zones, necessitating rigorous bias correction to align with in-situ measurements. The observed snow loss is driven by the snow-albedo feedback mechanism: the reduction of high-albedo snow cover exposes lower-albedo bedrock and regolith, thereby increasing the absorption of shortwave solar radiation and amplifying local near-surface heating. In high-elevation zones, this positive feedback loop drives warming rates of $0.50-0.67\,^{\circ}\mathrm{C\ decade}^{-1}$, significantly exceeding the global mean rate of $0.18\,^{\circ}\mathrm{C\ decade}^{-1}$ (Pepin et al., 2022).

Hydrological observations confirm that physical impacts are manifesting rapidly. Glacial-fed river basins exhibit altered discharge regimes, characterized by temporal shifts in the hydrograph. The Amu Darya river, a critical arterial water source for approximately 28 million inhabitants, shows a reduction in summer baseflow of 15%, while the centroid of the spring peak flow has advanced by 20–30 d. This regime shift necessitates a fundamental restructuring of agricultural planning and energy production strategies, which are currently calibrated to historical flow timing. Furthermore, projection heterogeneity suggests diverging hydrological futures: while northern Kazakhstan is projected to experience precipitation increases of 10–20%, southern Tajikistan faces potential deficits of 15% by mid-century, a spatial disparity that implies significant challenges for regional water allocation agreements (Fallah et al., 2024).

2.2.5 *Socio-Economic Implications of Hydro-Climatic Shifts*

The statistical trends in climatic variables translate directly into systemic socio-economic risks. The observed 27% reduction in glacial mass (Fallah et al., 2024) correlates with reduced irrigation reliability in the Fergana Valley, a region supporting 14 million people and intensive agricultural production. Similarly, the seven-fold increase in the frequency of meteorological droughts (Fallah et al., 2024) has destabilized pastoral systems in Kazakhstan, leading to livestock liquidation and economic loss for herding communities. Thermal extremes, characterized by heat waves reaching 48 °C (World Meteorological Organization, 2024), have necessitated the restructuring of labor practices, with construction and outdoor activities increasingly shifted to nocturnal schedules to mitigate heat stress risks.

Climate change in Central Asia thus represents a fundamental alteration of the boundary conditions within which regional societies have evolved. The decoupling of traditional ecological knowledge from observed environmental phenology creates a "knowledge gap" for agricultural management. Furthermore, the resilience of social networks, historically adapted to manage periodic resource scarcity, is being tested by the increased persistence of multi-year extreme events. The stationarity of the climate system–a core assumption for infrastructure design and resource planning–is effectively eroding.

The disaster statistics for 2023 (Fig. 2.3) provide a snapshot of this non-stationary risk landscape. The data indicate a trend where extreme events are increasing in frequency and magnitude. The challenge facing the region is not merely recovery from individual events but the implementation of adaptive strategies capable of keeping pace with a rapidly transforming climatic baseline.

2.3 Method

To ensure the physical plausibility of the projected scenarios, we had to account for both model uncertainty and the limitations of statistical downscaling techniques. Application of Super-Resolution Convolutional Neural Networks (SRCNN) has demonstrated useful skill in reconstructing historical high-resolution climates (Fallah et al., 2025). The application of such learning-based methods to far-future projections requires caution. Neural network architectures typically assume stationarity in the statistical relationships between large-scale predictors and local predictands. Under high-emission scenarios (e.g., SSP5-8.5), the climate system enters a "no-analogue" state where thermodynamical variables exceed the training domain of the network. Sensitivity analyses indicate that regression metrics (specifically R^2) for deep learning models can degrade by 40−60% when extrapolating to unprecedented extreme events (Fallah et al., 2025).

To mitigate this risk of extrapolation error while maintaining high spatial resolution, our long-term projections integrate the neural network approach with the

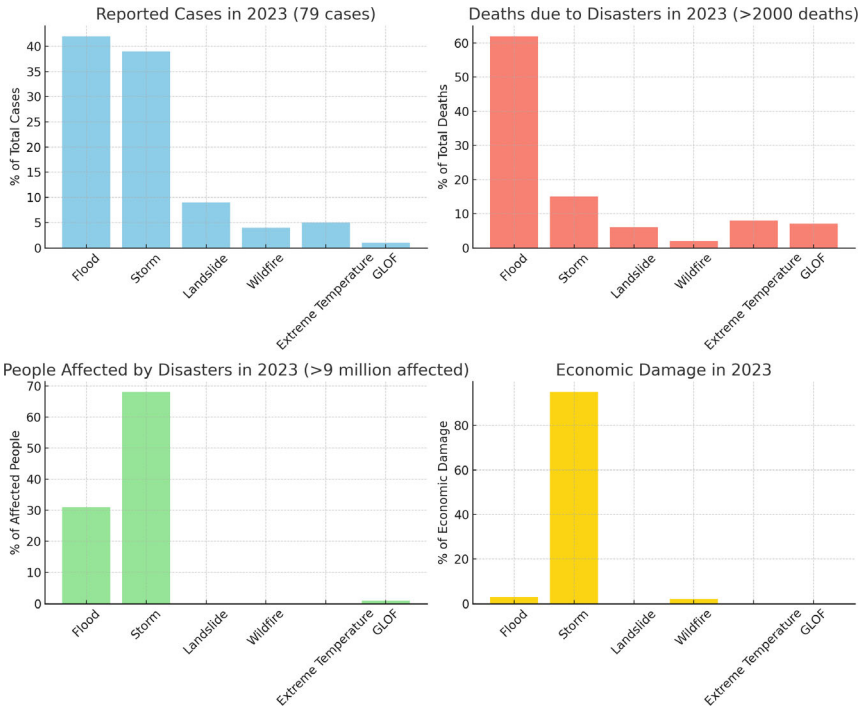


Fig. 2.3 Distribution of hydrometeorological disasters and associated impacts in Asia for the year 2023. The bar charts illustrate the frequency of events (top left), mortality (top right), population affected (bottom left), and economic damages (bottom right). Floods constituted the most frequent hazard (79 events), affecting 9 million individuals. *Source* Derived from WMO State of the Climate in Asia 2023 (World Meteorological Organization, 2024)

thermodynamic robustness of the NASA Earth Exchange Global Daily Downscaled Projections (NEX-GDDP-CMIP6). This dataset employs a Bias-Correction Spatial Disaggregation (BCSD) method that preserves the long-term trend signal of the parent General Circulation Models (GCMs) while correcting for local intensity distributions. This hybrid approach, combining machine learning for process understanding and bias-corrected GCM ensembles for future bounding, addresses the specific "extrapolation limitation" inherent in purely statistical approaches. The ensemble selection was harmonized with the Inter-Sectoral Impact Model Intercomparison Project (ISIMIP) protocols to ensure cross-sectoral consistency in impact assessment.

2.3.1 Ensemble Selection Criteria and Performance Validation

The projection ensemble consists of ten distinct Earth System Models (ESMs): GFDL-ESM4, IPSL-CM6A-LR, MPI-ESM1-2-HR, MRI-ESM2-0, UKESM1-0-LL, CNRM-CM6-1, BCC-CSM2-MR, INM-CM5-0, MIROC6, and EC-Earth3 (Fallah et al., 2025). This sub-selection from the broader CMIP6 archive was not arbitrary but determined through a rigorous "past-performance" evaluation metric. We validated the raw GCM outputs against ERA5 reanalysis data for the historical baseline period (1979–2014) (Hersbach et al., 2020). The selected models demonstrated superior skill at capturing the complex synoptic variability of the Central Asian domain, achieving spatial correlation coefficients (r) exceeding 0.85 for surface temperature and 0.70 for precipitation. This validation step is critical for establishing confidence in the models' ability to simulate the region's unique continental climatic drivers.

Despite their skill, raw GCM outputs exhibit systematic structural biases due to their coarse horizontal resolution (100–200 km), which necessitates correction. Topographic smoothing in the raw models results in a cold bias ranging from −2.3 °C to +3.2 °C, with the most significant errors observed in deep valleys where the model orography fails to resolve local lapse rates (Fallah, 2024). Precipitation fields similarly exhibit biases spanning −30 to +40%, typically characterized by the "drizzle effect" (overestimation of frequency/underestimation of intensity) on windward slopes and an under-representation of rain shadow aridity (Zhang & Wang, 2022). To address these systemic errors, we applied a Quantile Delta Mapping (QDM) bias-correction technique. This non-parametric approach adjusts the model distribution's quantiles to match the observed distribution, thereby reducing Root Mean Square Error (RMSE) by 60−70% for temperature and 40−50% for precipitation, effectively aligning the projection baseline with observed reality (Fallah et al., 2025).

2.3.2 Climate Sensitivity and Regional Amplification

A critical component of interpreting these projections is quantifying the region's specific sensitivity to radiative forcing. Central Asia is identified as a hotspot of climate change, characterized by warming rates that exceed the global mean. Our diagnostic analysis of the ensemble reveals a regional amplification factor ranging from 1.3 to 1.7 times the global average (Fallah et al., 2024). This amplification is quantified through the regional transient warming response, which averages 2.9 °C (ensemble range: 2.4−3.5 °C)–a value exceeding the global Transient Climate Response (TCR) by approximately 45%. Similarly, the regional equilibrium warming response reaches 4.3 °C (range: 3.6−5.2 °C) (Fallah & Rostami, 2024).

These sensitivity metrics indicate the dominance of strong positive feedback loops within the regional system, specifically the snow-albedo feedback and land-surface desiccation coupling. The physics governing these models dictate that once critical

moisture and cryospheric thresholds are crossed, warming accelerates non-linearly. The projection of a 6 °C rise is a physically consistent response to high radiative forcing within a highly sensitive continental system. The primary uncertainty in these projections lies not in the direction of the change, which is robust across all independent models, but in the rate of acceleration, which is determined by future emission pathways.

2.4 Projected Climatic Trajectories and Scenario Analysis

While observed trends demonstrate significant warming, future projections indicate a trajectory toward profound systemic transformation under high-emission scenarios. Utilizing a multi-model ensemble from the Coupled Model Intercomparison Project Phase 6 (CMIP6), statistically downscaled via advanced neural network architectures to a high spatial resolution of approximately 20–25 km (Fallah et al., 2025), our analysis indicates that Central Asia is entering a new climatic era, with temperatures likely to exceed any recorded in the region's history.

2.4.1 Scenario-Dependent Warming Pathways

Climate projections provide a range of probabilistic futures contingent upon global radiative forcing trajectories. Under the Shared Socioeconomic Pathway 1–2.6 (SSP1-2.6)–a sustainability scenario necessitating immediate and stringent mitigation of greenhouse gas emissions–Central Asia is projected to experience a mean surface temperature increase of 2.0–2.5 °C by 2100 relative to the pre-industrial baseline. While substantial, this magnitude of warming represents a "manageable" adaptation envelope. Conversely, under SSP5-8.5–a scenario characterized by high fossil fuel utilization and unmitigated emissions–warming is projected to reach approximately 6.1 °C (Fallah et al., 2024). Such a thermal excursion represents a fundamental state shift, potentially rendering current socio-ecological systems inviable.

The near-term trajectory (2021–2040) exhibits limited sensitivity to mitigation choices due to the inertia of the climate system; warming of 1.5–2.0 °C is considered *very likely* across all scenarios, driven by committed emissions. This inertia necessitates immediate adaptation planning for the coming two decades. However, the projection pathways diverge significantly in the mid-century period (2041–2060). While SSP1-2.6 stabilizes, SSP5-8.5 exhibits an accelerating trend, exceeding 3.5–4.5 °C (Fallah et al., 2024).

The implications of these thermal thresholds are non-linear. At 2 °C of warming, heat waves with a historical recurrence interval of 10 years are projected to become annual phenomena. At 4 °C, maximum temperatures currently classified as extreme anomalies would become the climatological mean for the summer season. Under the 6 °C scenario, large portions of the low-lying arid zones would experience wet-bulb

temperatures exceeding physiological tolerance thresholds for human habitation and outdoor labor during peak summer months.

2.4.2 Elevation-Dependent Warming (EDW) Mechanisms

A critical feature of regional climate sensitivity is Elevation-Dependent Warming (EDW), in which high-altitude regions exhibit higher warming rates than the lower troposphere. Our analysis indicates that warming rates above 3000 m exceed those at lower elevations by a factor of 1.5–3.0, with maximum amplification occurring in the 4000–5000 m hypsometric band (Pepin et al., 2022). In the Tien Shan range, this manifests as a vertical gradient in warming trends, with rates at lower elevations (1000–1500 m) significantly outpaced by those above 4000 m (Pepin et al., 2022).

This amplification is driven by a complex interaction of positive feedback mechanisms:

- **Snow-Albedo Feedback (SAF)**: Considered the dominant contributor to the total EDW signal (Pepin et al., 2015), this mechanism involves the melt of high-albedo snow cover, exposing lower-albedo substrate (rock and soil). This enhances the absorption of shortwave solar radiation, creating a self-reinforcing warming loop. The effect is most pronounced at the cryosphere-land transition zone, where seasonal snow cover is marginal.
- **Water Vapor Feedback**: A significant contributor to the amplification, this mechanism is driven by the Clausius-Clapeyron relationship. As the atmosphere warms, its capacity to hold water vapor increases. In high-altitude environments where the background specific humidity is low, small absolute increases in water vapor lead to disproportionately large increases in downward longwave radiation, trapping heat.
- **Cloud Feedback**: Also contributing to EDW, this involves the vertical displacement of cloud condensation levels. Warming shifts cloud formation upward, reducing the albedo effect at current glacier elevations while increasing the exposure of higher zones to insolation.

In the short term, EDW exhibits strong seasonal asymmetry. Winter shows the strongest amplification, driven primarily by SAF when solar incidence angles are low and snow cover extent is most sensitive to temperature. Spring shows moderate amplification associated with the acceleration of the melt season. Summer displays minimal EDW due to the absence of snow cover feedback (Pepin et al., 2022). This seasonality implies a “double negative” for water resources: enhanced winter warming suppresses snowpack accumulation, while spring warming accelerates ablation, effectively compressing the hydrological buffering window.

2.4.3 Phenological Shifts and Seasonal Asymmetry

The climatological seasonality that has historically governed regional agropastoral cycles is undergoing significant disruption. Winter temperatures are warming 20–30% faster than the annual mean, with high-emission projections indicating January anomalies of +7 to +8 °C by 2100 (Fallah et al., 2024). This trend threatens the viability of the cryospheric season as a distinct hydrological storage period. Projections indicate a potential decrease in Snow Water Equivalent (SWE) of 40−60% below 2000 m, accompanied by a shortening of the snow season by 30–45 d (Fallah, 2024).

The vernal transition (spring) is projected to become a period of increased variability. Warming rates 15–20% above the annual average, coupled with a 40–50% increase in inter-annual variability, creates stochastic risks (Fallah et al., 2024). This may manifest as "false springs"–early thermal pulses that trigger premature phenological development in February–followed by advective freeze events in April, causing catastrophic damage to agriculture. Conversely, years without freeze events may facilitate the proliferation of pests and pathogens.

Summer projections indicate the emergence of hyper-thermal regimes. Maximum temperatures exceeding 50 °C become statistically possible in lowland deserts. The frequency of days exceeding 40 °C is projected to increase substantially under high-emission scenarios (Fallah & Rostami, 2024). The duration of heat waves is also expected to increase, with extreme events potentially persisting for prolonged periods. Furthermore, the probability of compound heat-drought events is projected to increase, creating synergistic stressors on biological systems (Fallah et al., 2024).

The autumnal onset is projected to delay, extending the frost-free season by 20–30 d in the mountain zones and 30–40 d in the lowlands (Fallah et al., 2024). Although potentially increasing theoretical gross primary productivity, this extension exacerbates late-season water stress during the period of lowest hydrological baseflow and disrupts the dormancy cycles of perennial crops, which are essential for winter survival.

2.4.4 Hydrological Intensification and Cycle Acceleration

The intensification of the regional hydrological cycle constitutes the most consequential thermodynamic response to anthropogenic forcing in Central Asia. This acceleration is governed by the Clausius-Clapeyron relation, which dictates that the saturation vapor pressure of the atmosphere increases by approximately 6−7% for every 1 °C rise in temperature. Consequently, under high-emission scenarios (SSP5-8.5), the atmospheric water vapor capacity is projected to expand significantly by 2100. This thermodynamic priming intensifies moisture transport mechanisms, including Atmospheric Rivers (ARs)–narrow corridors of enhanced moisture flux. These synoptic features are increasingly important drivers of hydrological extremes, shifting the

operational paradigm of water management from steady-state allocation to extreme event mitigation (Zhang & Wang, 2022).

This intensification manifests as a profound non-stationarity in the frequency analysis of extreme events. The recurrence interval of the historical 100-year flood event is projected to contract substantially by mid-century under SSP5-8.5 forcing (Zhang & Wang, 2022). However, the most acute risk is associated with sub-daily precipitation intensity. Convective storms are projected to exhibit substantial increases in maximum rainfall intensity, generating flash flood pulses that exceed the hydraulic capacity of urban drainage and irrigation infrastructure designed for lower-energy climatic baselines (Zhang & Wang, 2022).

Paradoxically, this pluvial intensification occurs concomitantly with an expansion of meteorological drought conditions. The frequency of drought events is projected to increase by a factor of $2-3$, while the persistence of these anomalies extends from a typical duration of 3–6 months to multi-seasonal deficits lasting 12–18 months (World Meteorological Organization, 2024). This phenomenon, termed "precipitation whiplash," describes the rapid oscillation between extreme hydro-meteorological states–from severe moisture deficit to excess–rendering traditional reservoir storage strategies, which rely on predictable seasonal inflows, increasingly ineffectual.

Furthermore, the probability of "megadroughts"–defined as multi-year periods with precipitation deficits exceeding 40%–is shifting from a millennial-scale rarity to a centennial recurrence. Such events, historically occurring on millennial timescales, are projected to become substantially more frequent under high warming scenarios (Arias et al., 2021). Such a shift implies not merely a temporary deviation but a semi-permanent aridification of the baseline climate state, necessitating a fundamental restructuring of ecosystem services and agricultural dependencies.

2.4.5 Cryospheric Phase Transitions: The Rain-Snow Shift

The thermodynamic transition from solid to liquid precipitation represents a critical tipping point for the region's hydrology. The zero-degree isotherm (rain-snow transition zone) is projected to ascend at a rate of 165 ± 25 m per degree of warming. This vertical migration implies that by mid-century, a growing fraction of precipitation currently falling as snow will manifest as rain. This phase change drives a cascade of hydrological impacts: winter runoff volumes are projected to increase substantially due to immediate rainfall runoff, while summer baseflow–historically sustained by gradual snowmelt–is projected to decline (Tanrisever & Sakal, 2022).

For water resource management, this shift creates a "storage gap" crisis. Existing reservoir infrastructure, engineered to capture a predictable, high-volume spring snowmelt pulse, is ill-equipped to manage high-intensity winter rainfall events. Operators face a conflicting optimization problem: maintaining reservoir void space for winter flood control versus retaining storage for summer irrigation demand.

Traditional gravity-fed irrigation systems, calibrated to the historical timing of the meltwater hydrograph, face a binary risk profile: exposure to winter flood damage followed by acute summer supply deficits.

2.4.6 *Spatiotemporal Heterogeneity of Climate Signals*

The spatial manifestation of these climatic shifts reveals a complex pattern of regional divergence (Figs. 2.4 and 2.5). Temperature anomalies exhibit a distinct latitudinal and continental gradient, with amplification maxima located in the northern latitudes and within the desiccated Aral Sea basin, where surface albedo changes exacerbate local heating. Simultaneously, complex topographic effects amplify warming in high-elevation regions. Precipitation projections, however, display marked spatial fragmentation; adjacent catchment basins may exhibit opposing trends–some trending toward pluvial increases while neighbors face intensification of aridity. This

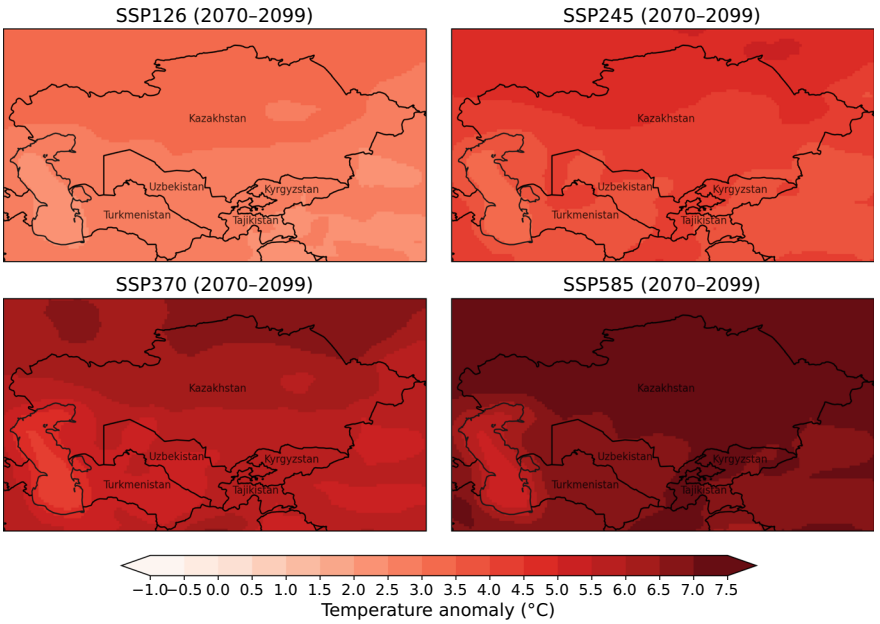


Fig. 2.4 Projected annual mean temperature anomalies (°C) for the period 2070–2099 relative to the 1995–2014 baseline, derived from the CMIP6 multi-model ensemble. Panels represent four Shared Socioeconomic Pathways (SSPs): SSP1-2.6 (top left), SSP2-4.5 (top right), SSP3-7.0 (bottom left), and SSP5-8.5 (bottom right). The spatial distribution highlights amplified warming in continental interiors and the Aral Sea basin (>7 °C under SSP5-8.5). Source: CMIP6 data downscaled by Fallah et al. 2024

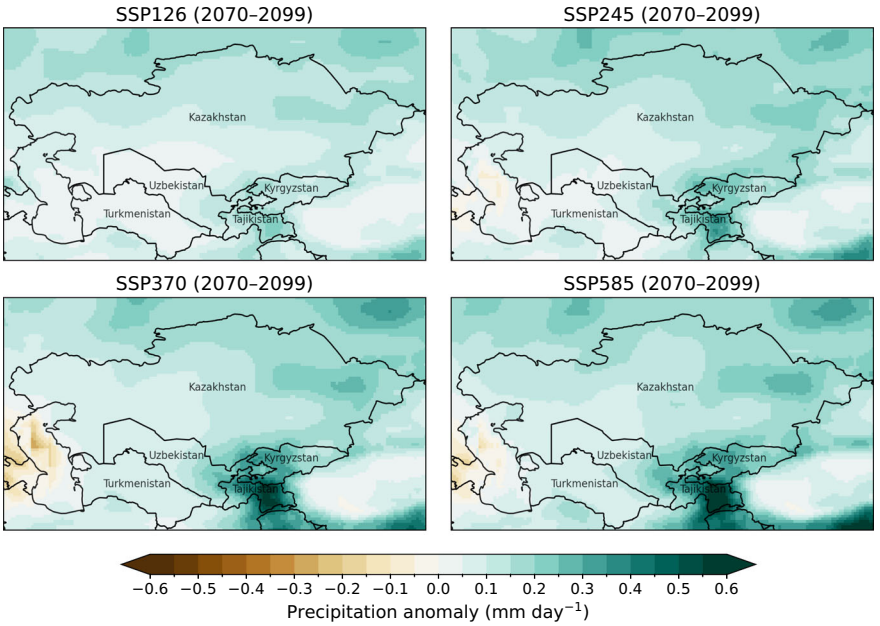


Fig. 2.5 Projected anomalies in daily precipitation rate (mm d^{-1}) for 2070–2099 under varying SSP scenarios. The maps illustrate significant spatial heterogeneity and uncertainty, with adjacent regions showing divergent wetting and drying trends. Note the complex orographic signal in the southeastern mountainous domains. *Source* CMIP6 data analysis (Zhang & Wang, 2022)

patchwork of hydrological outcomes complicates centralized planning and necessitates basin-specific adaptation strategies.

The temporal evolution of these variables introduces further complexity (Figs. 2.6 and 2.7). While the thermal trajectory is monotonic and scenario-dependent–diverging significantly after 2040–the precipitation signal shows increasing variance rather than a uniform shift in mean. The expansion of the uncertainty envelope over time reflects the inherent stochasticity of precipitation processes in a higher-energy atmosphere.

2.4.7 Projected Snowpack Depletion

The degradation of the seasonal snowpack represents the most critical threat to regional water security (Fig. 2.8). Under a 2 °C global warming scenario–considered a likely minimum boundary condition–Snow Water Equivalent (SWE) is projected to decline by 20−40% across the majority of the mountain domain. At 3 °C, these losses accelerate to 30−60%. Under a 4 °C warming scenario, the region enters a regime of cryospheric collapse, with projected losses of 40−80%, effectively eliminating the reliable seasonal snowpack below the 3500 m elevation contour.

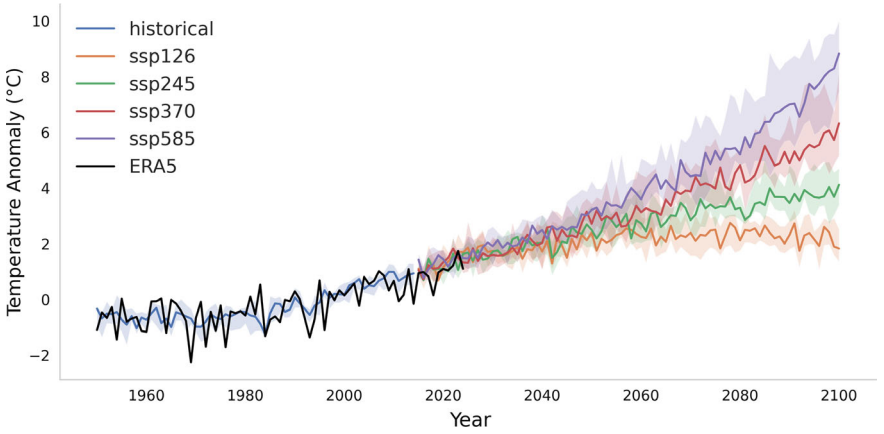


Fig. 2.6 Time series of annual temperature anomalies relative to the 1995–2014 baseline for Central Asia. The black line indicates ERA5 historical reanalysis data; colored plumes represent the multi-model ensemble spread (5th–95th percentile) across different SSP scenarios. A clear divergence in warming pathways is evident post-2040. *Source* Fallah et al. (2024)

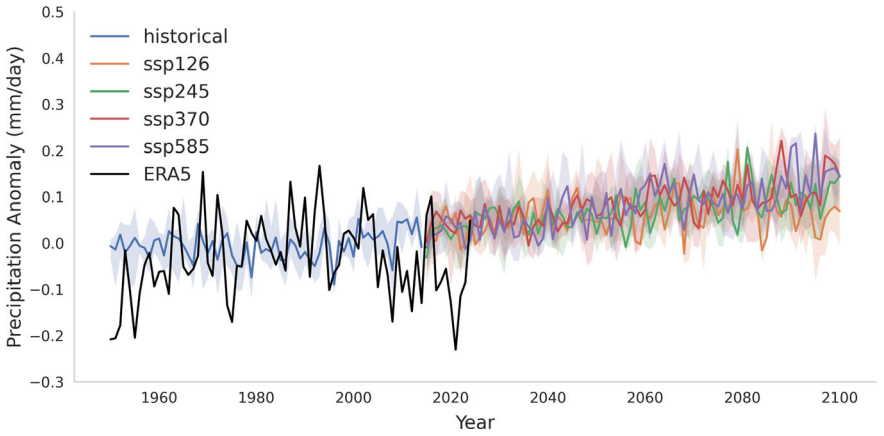
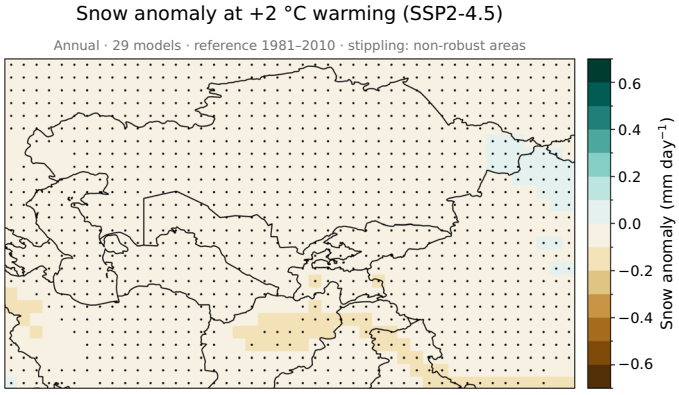
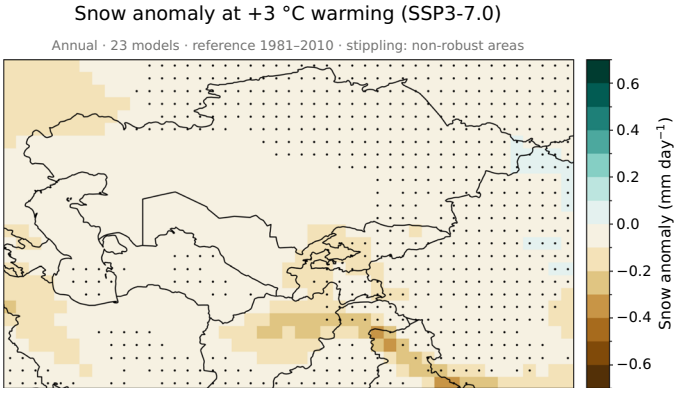


Fig. 2.7 Time series of annual precipitation anomalies relative to the 1995–2014 baseline. The expansion of the ensemble spread (shaded areas) over time indicates increasing inter-model uncertainty and internal climatic variability, distinct from the clear trend observed in temperature. *Source* Fallah et al. (2024)

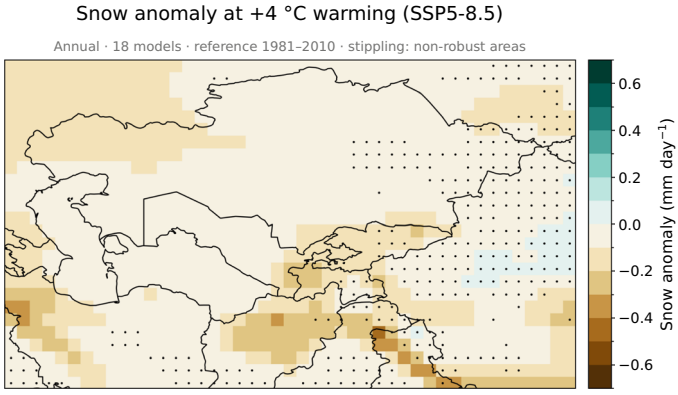
The mechanisms driving this loss are elevation-dependent. Below 2000 m, where ambient temperatures are proximal to the freezing point, even marginal warming induces rapid snowpack destabilization via three pathways: earlier onset of melt (advancing $10-15\,\mathrm{d}\,^{\circ}\mathrm{C}^{-1}$), increased rainfall-to-snow fraction (rising $20-30\%\,^{\circ}\mathrm{C}^{-1}$), and increased frequency of mid-winter ablation events. In the critical storage zone of 2000−3500 m, which currently holds 65% of the regional SWE,



(a) Snow anomaly at 2°C warming (approx. 2040s).



(b) Snow anomaly at 3°C warming (approx. 2060s).



(c) Snow anomaly at 4°C warming (approx. 2070s).

Fig. 2.8 Projected percentage change in Snow Water Equivalent (SWE) under varying global warming levels (2, 3, and 4 °C). Stippling indicates regions where > 80% of models agree on the sign of change, denoting high confidence in the drying signal. *Source* CMIP6 ensemble analysis (Fallah, 2024)

increased thermal variability facilitates frequent phase transitions during the accumulation season.

Threshold analysis indicates distinct regime shifts. At 2 °C warming, the ascent of the rain-snow line by 300−400 m compromises snow reliability for 12 million hectares of irrigated land. At 3 °C, the advance of the spring melt pulse by 35−45 d creates a temporal decoupling from peak agricultural demand. At 4 °C, the hydrology of 70% of currently snow-dominated basins transitions to a rain-dominated regime, characterized by a 150−200% increase in inter-annual storage variability and the normalization of multi-year snow droughts (Reyer et al., 2017; Fallah, 2024).

2.5 Strategies for Systemic Adaptation

Projections of 50−70% glacial mass loss by 2100 (Fallah et al., 2024) signal the end of the region's historical hydro-climate. The policy challenge has effectively shifted from preservation to managed transition; as the hydrological regime flips from snow-regulated to rain-dominated, the assumptions underpinning current infrastructure are becoming liabilities.

2.5.1 Engineering and Management Responses

Reservoir infrastructure faces a specific form of physical obsolescence: a mismatch between design parameters and shifting flow timing. Spring melt pulses now arrive 30–45 d earlier. Discharge magnitudes spike by 200−300% (Tanrisever & Sakal, 2022). Static storage cannot cope. Regional planners are therefore evaluating high-altitude retention basins. They are lining natural depressions with geomembranes to capture early runoff. Yet pilot data from the Kyrgyz Tien Shan suggest that such structures could substantially reduce peak flood discharge. This effectively converts a flood hazard into late-season irrigation storage.

Downstream inefficiencies worsen the supply crisis. Gravity-fed irrigation networks currently lose 40−60% of volume in transmission. These must be replaced with pressurized micro-irrigation systems capable of achieving 85% efficiency. Yet, modernization depends on the stability of the buffer resource: groundwater. Localized depletion rates in intensively pumped aquifers can reach 0.2–0.5 m/year. Kazakhstan has initiated Managed Aquifer Recharge (MAR) trials. These divert winter floodwaters into infiltration basins. As a result, piezometric levels have risen by 30−40%. This shows that flood risks can be repurposed for aquifer stabilization. Management frameworks must evolve, shifting from rigid annual quotas to real-time, sensor-based trading mechanisms that respond to daily volatility (Fallah et al., 2024).

2.5.2 Agricultural Restructuring and Economic Sensitivity

Agriculture faces the strictest physical boundaries. It consumes 85% of the regional water resources. Thermal forcing pushes optimal wheat cultivation zones upslope at 200–300 m per degree of warming. By 2050, this may force production systems to relocate across millions of hectares. Cotton production faces increasing thermal constraints, as rising temperatures are projected to push a growing share of current cultivation zones beyond physiological tolerance thresholds (Duenwald et al., 2022).

While technical adaptation pathways exist–including conservation tillage and drought-tolerant cultivars–the economic case for widespread adoption is shaped by both direct costs and broader fiscal impacts. Potential returns to adaptation can be substantial, with Benefit-Cost Ratios (BCR) ranging as high as 10:1, potentially avoiding 50−80% of climate damages (Duenwald et al., 2022). However, these figures are highly sensitive to discount rate assumptions, and shifting the social discount rate from 3% to 7% can substantially reduce the net present value of such projects, particularly for benefits accruing in the distant future. Moreover, formal economic models frequently overlook the region's substantial informal economy (30−50% of GDP), underrepresenting both the financial risks and adaptive capacity embedded in unmeasured and community-level responses (International Monetary Fund, 2023).

2.5.3 Ecological Services and Green Infrastructure

Natural systems function as non-substitutable critical infrastructure under changing climatic baselines. The projected upward migration of vegetation zones threatens a significant proportion of endemic taxa, underscoring the urgent need for assisted migration protocols. Alpine meadow ecosystems, which support millions of livestock units across the region, are projected to experience substantial productivity declines under drought conditions; however, implementing rotational grazing regimes and supplemental feeding can help stabilize carrying capacity (Xenarios et al., 2019).

Targeted restoration can mitigate impacts. Regional programs such as RESILAND Central Asia aim to restore degraded landscapes, sequester carbon, and reduce soil erosion, with land degradation costs estimated at 4% of GDP (World Bank, 2020). Restoration using drought-tolerant native species is a priority. In the Aral Sea basin, introducing halophytes to the exposed saline seabed can restore biomass and reduce toxic dust storms affecting downstream populations.

Urban green infrastructure yields major thermodynamic benefits: it reduces the urban heat island effect by 2−3 °C, attenuates stormwater, and cuts cooling energy needs by 15−20%. Urban greening initiatives in cities such as Bishkek have demonstrated favorable Benefit-Cost Ratios for climate adaptation investments (Fallah, 2024).

2.5.4 Integration of Traditional Ecological Knowledge (TEK)

The hybridization of Traditional Ecological Knowledge (TEK) with modern hydrological engineering offers cost-effective adaptation pathways. In Kyrgyzstan, traditional practices of artificial glaciation involve the construction of ice reservoirs in high-altitude valleys to enhance seasonal water retention. While historically community-managed, contemporary site selection optimization via geospatial modeling can maximize their hydrological efficiency (Xenarios et al., 2019).

Similarly, traditional stone-lined reservoirs for capturing vernal runoff have been shown to improve crop yields during drought years. Modern material upgrades (e.g., geomembranes) reduce seepage losses while preserving the decentralized governance structure essential for long-term maintenance. In the pastoral sector, traditional rotational grazing systems practiced in Kazakhstan reduce vegetative degradation relative to continuous grazing (Robinson et al., 2017); integrating such practices with satellite-derived biomass monitoring enables temporal optimization of herd movements (Xenarios et al., 2019).

The main challenge is formally integrating these indigenous methods into adaptation planning frameworks and scaling them through institutional recognition (World Bank, 2017).

2.6 Conclusion: Divergent Futures and Critical Thresholds

Central Asia has transitioned into a non-stationary climatic regime. The observed warming of 1.2 °C is not a precursor but a realized baseline; the shift to 2.0 °C is now thermodynamically committed. The divergence between a manageable future and systemic collapse lies in the trajectory beyond this threshold. Our analysis, synthesizing 442 model simulations (Fallah et al., 2024) and using high-resolution neural network downscaling (Fallah et al., 2025), confirms that regional climate sensitivity exceeds global averages, accelerating the approach to critical physical tipping points.

The scientific evidence delineates a stark bifurcation in potential outcomes. Under aggressive mitigation (SSP1-2.6), the region faces difficult but surmountable adaptation challenges: a 20−30% reduction in hydrological storage and manageable shifts in agropastoral zones.

Conversely, under high-emission pathways (SSP5-8.5), the region confronts a warming signal of 4−6 °C–a magnitude that breaches the physiological limits of current agricultural cultivars and the physical retention capacity of the cryosphere (Fallah & Rostami, 2024).

The difference between these scenarios is not merely incremental; it represents the boundary between adaptation and forced migration.

The decade preceding 2035 constitutes the definitive window for intervention. Decisions regarding water infrastructure modernization and transboundary cooperation made during this period will determine whether regional glaciers stabilize at 50% mass loss or proceed toward total deglaciation. Adaptation tools–ranging from artificial high-altitude reservoirs to drought-tolerant agronomic practices–are technically mature but financially constrained. Their deployment scale must match the rate of change of the hazard signal.

Ultimately, the future of Central Asia will be defined by the "adaptation gap"–the lag between the rate of climatic forcing and the implementation of resilient infrastructure. The data indicate that while physical transformation is inevitable, the societal magnitude of this crisis remains mutable. The preservation of the region's socio-economic viability requires that policy frameworks immediately align with the physical realities of a rapidly warming continent (Tables 2.1 and 2.2).

Table 2.1 Summary of observed and projected climate impacts in Central Asia

Impact category	Observed changes	Projected changes (2100)
Physical impacts	Temperature: +1.5°C (1880–2020), significant agricultural disruption; Precipitation: ±30% regional variation, concurrent drought and flooding; Snow cover: −20% (1950–2020), viability of winter tourism significantly reduced	Temperature: +2–6°C (SSP dependent), livability thresholds exceeded; Precipitation: −15% to +10%, increased risk of transboundary water conflict; Snow cover: −40–70%, snow-fed rivers transition to seasonal regimes
Water resources	Glacier mass: −27% (1961–2020), critical storage capacity declining; River flow: −15% summer baseflow, irrigation reliability reduced; Groundwater: −2 m average decline, aquifer depletion accelerating	Glacier mass: −50–70%, sustained water supply crisis; River flow: −30–60% summer, irrigation system failure; Groundwater: −5–8 m, widespread aquifer exhaustion
Ecosystem	Vegetation zones: 200–500 m upward shift, increased forest mortality; Growing season: +15–25 d, offset by thermal stress; Fire frequency: +40%, extended fire seasons	Vegetation zones: 500–1000 m shift, large-scale ecosystem displacement; Growing season: +30–45 d, heat stress dominant; Fire frequency: +100–150%, near-permanent fire risk
Extreme events	Heatwaves: +50% frequency, severe public health burden; Droughts: 7× increase since 1950, widespread livelihood disruption; GLOFs: numerous dangerous lakes, heightened downstream vulnerability	Heatwaves: substantial frequency increase, outdoor labor capacity severely reduced; Droughts: further intensification, semi-permanent aridification; GLOFs: 400+ dangerous lakes, critical risk to valley populations

Table 2.2 Current status of climate monitoring and projection systems for Central Asia

Category	Current infrastructure	Operational capabilities
Observation networks	Weather stations: 450 active, 40% manual operation; Glacier monitoring: 85 high-altitude sites; Hydrological gauges: 320 stations, subject to operational challenges	60% automated, enabling real-time drought monitoring; 30% real-time data transmission for flood alerts; 15% with telemetry, supporting early warning systems
Climate models	CMIP6 downscaling: 20 km resolution, basin-specific projections; Regional models: WRF, RegCM for local extremes; Neural network downscaling (Fallah et al., 2025)	5 models operational, providing decision-ready projections; 2 peer-reviewed studies published; First neural network application in the region
Projections	Temperature: ensemble mean with quantified confidence; Precipitation: multi-model spread with uncertainty bounds; Extremes: attribution studies establishing anthropogenic contribution	SSP1-2.6 to SSP5-8.5 scenarios fully characterized; 2030–2100 timeframe for long-term planning; 95% confidence intervals for risk assessment
Early warning	Flood forecasting: 72 h lead time; Drought monitoring: SPEI and SPI indices; Heat wave alerts: 5 d forecast horizon	65% accuracy, statistically significant skill; ML integration planned, targeting 80% accuracy; Multi-hazard platform under development

References

Arias, P. A., et al. (2021). Technical summary. In V. Masson-Delmotte & P. Zhai, et al. (Eds.), *Climate change 2021: the physical science basis: Contribution of working group i to the sixth assessment report of the intergovernmental panel on climate change* (pp. 33–144). Cambridge University Press: Cambridge, United Kingdom and New York, NY, USA.DOI: 10.1017/9781009157896.002.

Chen, F., et al. (2019). Westerlies Asia and monsoonal Asia: Spatiotemporal differences in climate change and possible mechanisms on decadal to sub-orbital timescales. *Earth-Science Reviews, 192*, 337–354.

Didovets, I., et al. (2024). Attribution of current trends in streamflow to climate change for 12 central Asian catchments. *Climatic Change, 177*(1), 16.

Duenwald, C., et al. (2022). Feeling the heat: Adapting to climate change in the middle east and central Asia. Departmental Paper DP/2022/008. International Monetary Fund.

Fallah, B. (2024). High-resolution CMIP6 analysis highlights emerging climate challenges in alpine and Tibetan Tundra zones. *Meteorological Applications, 31*(5), e70001. https://doi.org/10.1002/met.70001

Fallah, B. & Rostami, M. (2024). Exploring the impact of the recent global warming on extreme weather events in central Asia using the counterfactual climate data ATTRICI v1.1. *Climatic Change, 177*(5), 80. https://doi.org/10.1007/s10584-024-03743-0

Fallah, B., & Saberi, A. A. (2016). Emergence of global scaling behaviour in the coupled Earth-atmosphere interaction. *Scientific Reports, 6*, 34005. https://doi.org/10.1038/srep34005

Fallah, B., et al. (2023). Anthropogenic influence on extreme temperature and precipitation in central Asia. *Scientific Reports, 13*(1), 6854. https://doi.org/10.1038/s41598-023-33921-6

Fallah, B., et al. (2024). Climate change impacts on central Asia: Trends, extremes and future projections. *International Journal of Climatology, 44*(10), 3191–3213. https://doi.org/10.1002/joc.8519

Fallah, B., et al. (2025). Climate model downscaling in central Asia: A dynamical and a neural network approach. *Geoscientific Model Development, 18*(1), 161–180. https://doi.org/10.5194/gmd-18-161-2025

Farinotti, D., et al. (2015). Substantial glacier mass loss in the Tien Shan over the past 50 years. *Nature Geoscience, 8*(9), 716–722. https://doi.org/10.1038/ngeo2513

Fu, Q., & Lin, P. (2011). Poleward shift of subtropical jets inferred from satellite-observed lower-stratospheric temperatures. *Journal of Climate, 24*(21), 5597–5603. https://doi.org/10.1175/JCLI-D-11-00027.1

Guo, H., et al. (2021). Assessment of CMIP6 in simulating precipitation over arid central Asia. *Atmospheric Research, 252*, 105451. https://doi.org/10.1016/j.atmosres.2021.105451

Hassanabadi, B. F. (2015). Modelling the Asian paleo-hydroclimatic variability. Ph.D. thesis. Freie Universität Berlin. https://www.fu-berlin.de/en/sites/studium/abschlussarbeiten/download/thesis/hassanabadi2015_modelling.pdf.

Hersbach, H., et al. (2020). The ERA5 global reanalysis. *Quarterly Journal of the Royal Meteorological Society, 146*(730), 1999–2049.

International Monetary Fund. (2023). Regional economic outlook: Middle east and central Asia – Building resilience in challenging times. Technical report see specifically Chapter 2 on fiscal risks and the informal economy estimates (30–50% of GDP in Central Asia). Washington, DC: International Monetary Fund. https://doi.org/10.5089/9798400237678.086

Lambrecht, A., et al. (2014). The evolution of Fedchenko glacier in the Pamir, Tajikistan, during the past eight decades. *Journal of Glaciology, 60*(220), 233–244. https://doi.org/10.3189/2014JoG13J110

Pepin, N., et al. (2015). Elevation-dependent warming in mountain regions of the world. *Nature Climate Change, 5*(5), 424–430. https://doi.org/10.1038/nclimate2563

Pepin, N. C., et al. (2022). Climate changes and their elevational patterns in the mountains of the world. *Reviews of Geophysics, 60*(1), e2020RG000730.

Reyer, C. P. O., et al. (2017). Climate change impacts in central Asia and their implications for development. *Regional Environmental Change, 17*(6), 1639–1650. https://doi.org/10.1007/s10113-015-0893-z

Robinson, S., et al. (2017). Pastoralists as optimal foragers? Reoccupation and site selection in the deserts of post-Soviet Kazakhstan. *Human Ecology, 45*(2), 149–171. https://doi.org/10.1007/s10745-016-9870-5

Tanrisever, O. F., & Sakal, H. B. (Eds.). (2022). *Water, energy and environment in Eurasia*. Nevsehir: Cappadocia University Press.

World Bank. (2020). RESILAND CA+: Resilient landscape restoration in central Asia. Technical report workshop presentation. Landscape restoration program for central Asia (p. 2020). Washington, DC: World Bank.

World Bank. (2017). Tajikistan: glass half full - poverty diagnostic. World bank group. Technical report. https://doi.org/10.1596/978-1-4648-1048-0

World Meteorological Organization. (2024). State of the Climate in Asia 2023. Technical report WMO-No. 1302. Geneva, Switzerland: World Meteorological Organization.

Xenarios, S., et al. (2019). Climate change and adaptation of mountain societies in central Asia: Uncertainties, knowledge gaps, and data constraints. *Regional Environmental Change, 19*(5), 1339–1352. https://doi.org/10.1007/s10113-018-1384-9

Xinhua. (2023). Uzbekistan prepares for another heatwave. Citing forecasts from the Center of Hydrometeorological Service of Uzbekistan (Uzhydromet). Retrieved December 17, 2025, from https://english.news.cn/asiapacific/20230724/761c17fdafd6429ea0b0c4b8f6590fde/c.html

Zhang, J., & Wang, F. (2022). Future changes in extreme precipitation in central Asia with 1.5–4 C global warming based on coupled model intercomparison project phase 6 simulations. *International Journal of Climatology, 42*, 8509–8525.

Open Access This chapter is licensed under the terms of the Creative Commons Attribution 4.0 International License (http://creativecommons.org/licenses/by/4.0/), which permits use, sharing, adaptation, distribution and reproduction in any medium or format, as long as you give appropriate credit to the original author(s) and the source, provide a link to the Creative Commons license and indicate if changes were made.

The images or other third party material in this chapter are included in the chapter's Creative Commons license, unless indicated otherwise in a credit line to the material. If material is not included in the chapter's Creative Commons license and your intended use is not permitted by statutory regulation or exceeds the permitted use, you will need to obtain permission directly from the copyright holder.

